Macromolecules
Cite This: Macromolecules 2019, 52, 8967−8975
Article
pubs.acs.org/Macromolecules

Tuning Mechanical Properties of Biobased Polymers by Supramolecular Chain Entanglement

Meghan E. Lamm,[†] Lingzhi Song,[‡] Zhongkai Wang,[‡] Md Anisur Rahman,[†] Benjamin Lamm,[†] Lin Fu,[†] and Chuanbing Tang*[,†]

[†]Department of Chemistry and Biochemistry, University of South Carolina, Columbia, South Carolina 29208, United States
[‡]Biomass Molecular Engineering Center, Anhui Agricultural University, Hefei, Anhui 230036, China

Supporting Information

ABSTRACT: A variety of biobased polymers have been derived from diverse natural resources. However, the mechanical properties of some of these polymers are inferior due to low chain entanglement. We report a facile strategy termed "supramolecular chain entanglement", which utilizes supramolecular interactions to create physical cross-linking and entanglements for polymers with long pendent fatty chains. The ensuing bioplastics—prepared by mixing copolymers, composed of a plant oil-derived methacrylate with an acid-containing comonomer as a hydrogen-bonding donor—and poly(4-vinylpyridine) as an entangling chain with a hydrogen-bonding acceptor show tunable mechanical strength and toughness. These polymer blends, consisting of ≥90 wt % sustainable sources, exhibit marked improvement in thermomechanical properties compared with the viscoelastic nature of the biobased homopolymers. Spectroscopic evidence and X-ray scattering substantiated the hydrogen-bonding interaction within the copolymers, while morphological and thermal characterization was performed to elucidate microstructures of biobased polymers.

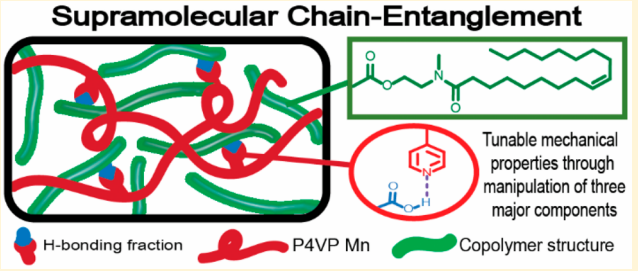

INTRODUCTION

Recent research thrusts on the use of renewable resources intensify efforts to pursue the manufacture of bioplastics.[1−9] Nevertheless, sustainable polymers face many challenges, including high cost and poor performance, which limit their competitiveness in the current market. These issues could be mitigated by using common, cheap biomass sources coupled with minimal or highly efficient functionalization.[10−12] For example, plant oils with a global production of nearly 200 million tons are a promising renewable resource for making biobased polymers with additional benefits of low cost and value-added functionality.[1,13−17]

However, many of these bioplastics have poor mechanical properties, including fragility and low strength. Derived from a variety of biomass, these polymers could possess bulky or long pendent chains, which can result in significantly lower chain entanglement (and therefore high entanglement molecular weight, M_e).[18] M_e is very high for polymers with bulky side groups from biomass such as soybean oil (>200 kDa), rosin acids (>90 kDa), and terpenes (>30 kDa).[19−21] A few strategies have been developed to overcome high M_e: (1) the use of ultrahigh molecular weight polymers,[20] (2) utilization of chain architectures such as block copolymers to allow for stress dissipation,[19,21−27] and (3) incorporation of physical or dynamic chemical cross-linking to induce chain entanglement.[27−29] Dynamic cross-linking is a viable approach with the aid of a wide variety of chemistries such as supramolecular interactions and exchangeable bonding. Supramolecular interactions such as hydrogen bonding (H-bonding) have been widely used as dynamic bonds to improve properties of polymers.[30−41]

Herein we report a simple, yet robust "supramolecular chain entanglement" strategy for the creation of physical cross-linking and entanglements to substantially enhance mechanical properties of biomass-derived polymers, as illustrated in Figure 1. We present plant oils as a biomass origin to demonstrate the validity of this concept. Specifically, we introduce H-bonding into a polymeric system to induce physical cross-links. Acidic proton donors (e.g., carboxylic acids) and basic proton acceptors (e.g., amines and pyridines) are among the most desirable H-bonding pairs due to their high affinity, good precursor solubility, and facile availability.[42,43] In this work, commercial carboxylic acids such as methacrylic acid (MAA), acrylic acid (AA), and 2-carboxyethyl acrylate (CEA) were used as H-bonding donor comonomers, which were introduced into soybean oil-derived polymers via radical copolymerization. The copolymers were then mixed with poly(4-vinylpyridine) (P4VP), an H-bonding acceptor. The H-bonding interactions between pyridine and acid units would create physical cross-links among bulky biomass-derived polymers and further enable the chains of P4VP to wrap around them.

Received: September 2, 2019
Revised: October 28, 2019
Published: November 13, 2019

DOI: 10.1021/acs.macromol.9b01828
Macromolecules 2019, 52, 8967−8975

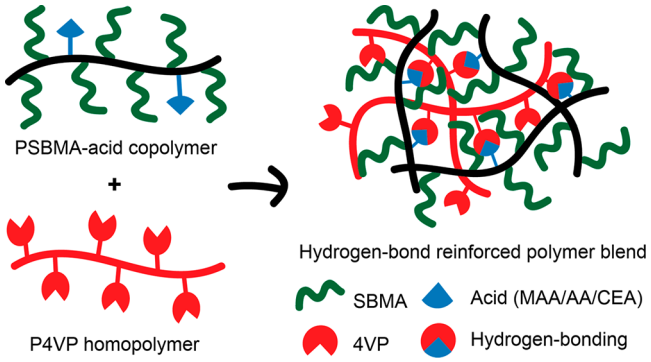

Figure 1. Graphical illustration of "supramolecular chain entanglement": P4VP is used as H-bonding acceptors to interact and wrap soybean oil-based copolymers containing H-bonding acidic donors, which produces physical cross-links toward more efficient chain entanglements.

A few design principles guide the macromolecular compositions: (1) The entangling polymers should be readily processable and have a relatively low M_e with functionalities to facilitate the formation of physical cross-links. P4VP could meet these criteria with its M_e at ∼30 kDa.[18] (2) Biomass monomers should be able to copolymerize with other monomers that are not only low cost and commercially available but also able to induce supramolecular interactions with the entangling polymers. Thus, carboxylic acid-based (meth)acrylate monomers would be a good choice. (3) The biomass content should be aimed at sustainability; in other words, the entangling polymers and those for supramolecular interactions should be used at the minimum level.

RESULTS

Preparation of H-Bonded Polymer Blends. Soybean oil-based copolymers were synthesized by using free radical copolymerization of soybean monomers and carboxylic acid monomers (Scheme 1). Large-scale synthesis of soybean methacrylate (SBMA) monomer was recently demonstrated.[44] However, the SBMA homopolymer (PSBMA) is a viscoelastic liquid.[45,46] The addition of a small fraction (≤5 wt %) of acid-based comonomers successfully transformed the viscoelastic homopolymer to a thermoplastic copolymer. This is substantial in terms of the effect of comonomers on mechanical properties. To examine the effect of acid contents, copolymers of each acid system with two different weight fractions of acid (2 and 5 wt %) were prepared (copolymer named with acid monomer and its weight percentile, Table 1). First, MAA-containing copolymers suffer from brittleness, mostly due to the high-T_g nature of the MAA polymer (PMAA T_g ∼ 230 °C). Therefore, a comparative system with a softer AA component was utilized (PAA T_g ∼ 106 °C). As both MAA and AA units are much smaller than bulky SBMA, the acid units are likely surrounded by pendant fatty side chains, potentially limiting the formation of H-bonding.[47] Thus, CEA-containing copolymers were synthesized. CEA is a soft acid monomer (PCEA T_g ∼ 30 °C), bearing a longer pendant carboxylic group.

Table 1. Characterization Data of PSBMA Homopolymer, P(SBMA-*co*-MAA) Copolymers (MAA2 and MAA5), P(SBMA-*co*-AA) Copolymers (AA2 and AA5), and P(SBMA-*co*-CEA) Copolymers (CEA2 and CEA5)

sample code	acid content[a] (wt %)	acid content[a] (mol %)	T_g[b] (°C)	M_n[c] (kDa)	$Đ$[c]
PSBMA	0	0	−6	43.4	1.78
MAA2	2	8.8	19	83.5	2.49
MAA5	5	20.0	35	81.3	2.21
AA2	2	10.3	−4	29.4	2.70
AA5	5	22.9	−2	32.9	2.98
CEA2	2	5.5	−6	33.4	2.66
CEA5	5	12.9	−5	32.9	2.64

[a]Weight and molar fractions of MAA, AA, and CEA were calculated based on ^{1}H NMR. [b]T_g values were obtained by DSC (second heating cycle). [c]Molecular weight and molecular weight distribution were characterized via GPC.

All copolymers were characterized by ^{1}H NMR (Figure S1). Because of the difference in monomer reactivity, the molecular weights of AA and CEA copolymers are much lower than those of MAA copolymers. Compared to the glass transition temperature (T_g) of the **PSBMA** homopolymer (−6 °C), a significant increase was observed for MAA copolymers, 19 °C for **MAA2** and 35 °C for **MAA5**, whereas a minimal change in

Scheme 1. Synthesis of Soybean Oil-Based Methacrylate Monomers from High Oleic Soybean Oil and Soybean Oil-Based Copolymers P(SBMA-*co*-MAA/AA/CEA) via Free Radical Copolymerization

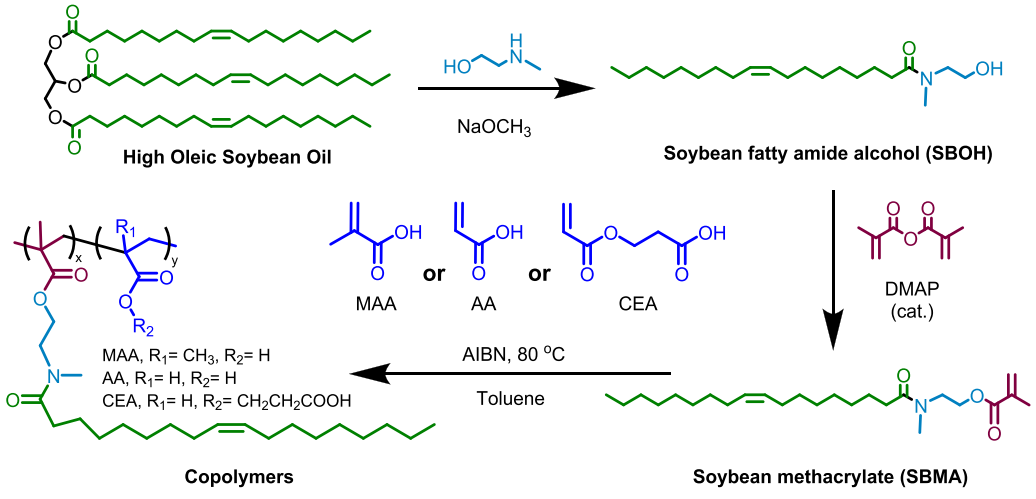

DOI: 10.1021/acs.macromol.9b01828
Macromolecules 2019, 52, 8967−8975

T_g was observed for AA and CEA copolymers (T_g < −2 °C). The weight and molar fractions of comonomers in the resulting copolymers were calculated based on feed ratios and conversion of comonomers in the crude reaction mixture after polymerization, both confirmed by ^{1}H NMR (Table 1).

Supramolecular polymer blends were prepared by solution mixing of soybean copolymers and P4VP. P4VP was synthesized using reversible addition−fragmentation transfer (RAFT) polymerization, following an established procedure.[48] Three P4VP polymers with different molecular weights were synthesized (M_n = 8, 30, and 60 kDa) (Figure S2). All blends used the following naming system: the copolymer name indicating the acid monomer and its weight fraction in number (**MAA2**, **MAA5**, **AA2**, **AA5**, **CEA2**, or **CEA5**) and P4VP following by a number indicating its weight fraction. The number in parentheses refers to as the molecular weight P4VP. For example, blend **MAA5-P4VP2 (30K)** contains MAA-based copolymer with 5 wt % MAA and 2 wt % P4VP with M_n = 30 kDa. Molar and weight fractions of all components in each polymer blend are shown in Table S1. To maintain high sustainability, all blends contain ≥90 wt % of soybean monomer, while the fractions of acid monomer (MAA, AA, or CEA) and 4VP together are ≤10 wt %. All polymer blends formed free-standing films, a remarkable mechanical improvement compared to the tacky PSBMA homopolymer.

As H-bonding is sensitive to temperature, variable-temperature FTIR was employed to probe its presence in the blend system for understanding the effect of supramolecular interactions on microstructures.[42,43,47,49] As shown in Figure 2a and Figure S3, three peaks were tracked: N···H, bonded C═O in amide, and free C═O in amide. At lower temperature, an N···H peak (1608 cm^{-1}) appeared due to the delocalization of the carbonyl as a result of H-bonding with the pyridine group. This peak decreases in intensity with the increase of temperature, indicating the weakening of H-bonding. Additionally, tertiary amide groups from the SBMA units also participate in the H-bonding. They serve as H-bonding acceptors, in which the carbonyl bond was observed with a shift in its peak position, with a lower peak (1650 cm^{-1}) present at lower temperature, which corresponds to the associated H-bonding amide, and a higher peak (1654 cm^{-1}) present at higher temperature, which corresponds to the dissociated moiety not participating in H-bonding. There is also a correlation between all these peaks which show trends in peak intensity for N···H, free C═O, and bonded C═O as a function of temperature (Figure 2b).

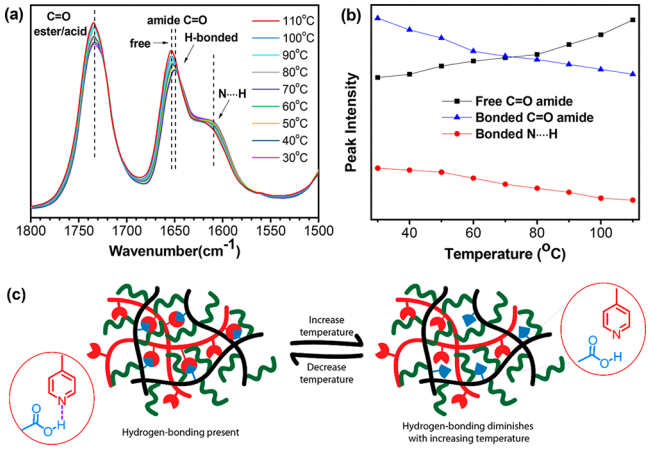

Figure 2. (a) Variable temperature FTIR spectra of a representative polymer blend (**MAA5-P4VP5 (60K)**) at various temperatures. (b) Peak intensity of different bonds involving H-bonding as a function of temperature. (c) A proposed microstructure of polymer blends during heating and cooling cycles.

Additional characterization on probing H-bonding interactions was performed using solid-state ^{13}C CP-MAS NMR. It has been reported that carboxylic acid can undergo dimerization, which can be disrupted by the addition of pyridine due to the formation of stronger hydrogen bonding between acid and pyridine.[50] In this work, an MAA copolymer with a higher faction of MAA (molar ratio of SBMA:MAA at 1:1) was synthesized to amplify acid peaks from those of aliphatic backbone and side chain. This copolymer was blended with **P4VP-60** to give a final molar ratio of SBMA:MAA:4VP around 1:1:1. Using ^{13}C NMR, we compared the copolymer and blend (Figure S4). For the copolymer there is a broad peak around 172 ppm, representing the ester and amide carbonyls. An additional smaller peak at 182 ppm corresponds to the acid carbonyl. This peak location is consistent with the dimerization of carboxylic acid as reported in the literature.[50] The blend only exhibits one broader peak at 173 ppm, while the peak at 182 ppm completely disappeared. This indicates that the acid is no longer dimerized, most likely due to the new interaction between acid and pyridine. Taken together with FTIR results, it is evident that there is a presence of complex supramolecular interactions within 4VP, SBMA, and MAA units through H-bonding.

Further morphological data were obtained by using small-angle X-ray scattering (SAXS). At room temperature (25 °C), only one broad peak is present corresponding to a *d*-spacing of 3−3.8 nm (Figure S5a), which is consistent with previously reported ill-defined side-chain packing of pendant fatty chains.[23] The lack of high orders of scattering peaks at low *q* values indicates the absence of phase separation, further suggesting that the polymer blends are miscible. We further performed SAXS experiments to track phase separation of the blend system at various temperature (Figure S5b). Once heated from 40 to 100 °C, the SAXS profiles show the emergence of a new peak associated with a larger correlation length (~8.5 nm), suggesting that there might be some weak phase separation though it is not clear what this peak represents for. It could be explained by the disruption of H-bonding and thus gradual increase of immiscibility. Further heating to 140 °C resulted in the disappearance of the newly formed peak, most likely due to the "order−disorder" transition that is commonly associated with temperature-dependent Flory−Huggins parameter (it is beyond the scope of this work to carry out quantitative analysis). However, after cooling to room temperature, the SAXS profile is almost identical to the one before heating, mostly likely due to the recovered H-bonding and therefore good miscibility. Based on these results, a proposed microstructure model is illustrated in Figure 1, where chains of soybean copolymer and P4VP are favorably entangled, facilitated by supramolecular interactions between carboxylic acid groups in the copolymer and pyridine groups in P4VP. The formation of H-bonding-based physical networks can dissipate stress from one macromolecule to another, thus potentially changing physical properties over the viscoelastic homopolymers. Varying the compositions of H-bonding moieties and chain flexibility could allow for tailorable

DOI: 10.1021/acs.macromol.9b01828
Macromolecules 2019, 52, 8967−8975

Table 2. Mechanical Properties of H-Bonded Polymer Blends with Varied Molecular Weights of P4VP[a]

sample code (wt %)	M_n (Da) (P4VP)	T_g[b] (°C)	stress at break (MPa)	strain at break (%)	toughness (MJ/m^3)	storage modulus at 25 °C (MPa)
MAA2-P4VP2 (8K)	8000	19	0.7 ± 0.03	408 ± 9	3.2 ± 0.3	8.6
MAA2-P4VP5 (8K)	8000	22	0.7 ± 0.05	391 ± 14	2.6 ± 0.3	
MAA5-P4VP2 (8K)	8000	38	5.1 ± 0.3	18 ± 2	0.6 ± 0.1	
MAA5-P4VP5 (8K)	8000	42	3.1 ± 0.2	91 ± 13	3.3 ± 0.1	199
MAA2-P4VP2 (30K)	30000	20	3.6 ± 0.05	300 ± 13	10.1 ± 0.3	51
MAA2-P4VP5 (30K)	30000	23	5.1 ± 0.1	290 ± 9	14.5 ± 0.3	
MAA5-P4VP2 (30K)	30000	39	8.0 ± 0.4	75 ± 2	5.3 ± 0.1	
MAA5-P4VP5 (30K)	30000	43	11.6 ± 0.3	14 ± 0.5	1.2 ± 0.0	202
MAA2-P4VP2 (60K)	60000	20	2.3 ± 0.02	474 ± 22	9.9 ± 0.4	31
MAA2-P4VP5 (60K)	60000	24	4.7 ± 0.05	267 ± 14	11.1 ± 0.2	
MAA5-P4VP2 (60K)	60000	39	12.0 ± 0.4	16 ± 0.5	1.2 ± 0.0	
MAA5-P4VP5 (60K)	60000	43	17.0 ± 0.9	7 ± 0.2	0.8 ± 0.0	390

[a]All blends use the following naming system: the copolymer name indicating the acid monomer and its weight fraction in number (**MAA2** and **MAA5**) and P4VP following by a number indicating its weight fraction. The number in parentheses refers to as the molecular weight P4VP. [b]T_g values were obtained via DSC (second heating cycle).

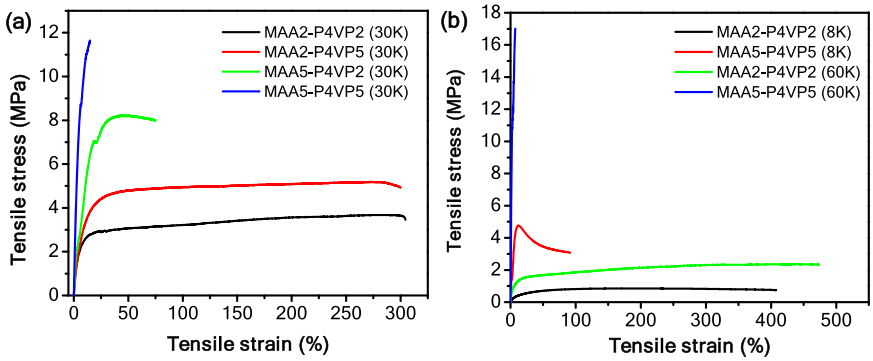

Figure 3. Stress–strain curves of polymer blends with variation in compositions: (a) variation in H-bonding fractions; (b) variation in molecular weight of P4VP.

bioplastics that have mechanical improvement compared to soybean oil-based homopolymers.

Mechanical Properties. A major goal of this work was to demonstrate that supramolecular chain entanglement could be tuned for direct control of mechanical properties. By changing chemical compositions, including the level H-bonding, the molecular weight of chain entangling polymer, and chain flexibility, the direct effect of variations in macromolecular composition on thermomechanical properties can be elucidated.

We first chose P4VP with M_n = 30000 Da as a model H-bonding acceptor polymer for making polymer blends, as this molecular weight is close to M_e of P4VP. To examine the effect of H-bonding components on mechanical properties of polymer blends, we varied the overall weight ratios of H-bonding monomeric units, which are maintained ≤10 wt % to maximize the sustainable component of soybean (Table 2 and Figure 3a). Via increasing H-bonding weight fractions from 4% to 10% with MAA:4VP at 1:1, the tensile strength increased from 3.6 to 11.6 MPa, while the strain at break decreases from 300% to 14%, indicating the dramatic impact of H-bonding on the blends. With the same total fractions of H-bonding components (**MAA5-P4VP2 (30K)** vs **MAA2-P4VP5 (30K)**), the more the MAA (**MAA5-P4VP2 (30K)**), the stronger the blend. This could be partially due to the existence of H-bonding among carboxylic acid units, which 4VP units do not possess. In addition, a series of dynamic mechanical analysis (DMA) experiments showed that blends with higher H-bonding content (10 wt %) had the highest storage modulus at 25 °C (Figure S6), consistent with the tensile tests.

We then explored two other P4VP homopolymers with different molecular weights: M_n = 8000 Da and M_n = 60000 Da, which are respectively below and above the M_e of P4VP. In the case of $M_n \ll M_e$, the blends with both low and high fractions of H-bonding components exhibited very low tensile strength (<3–5 MPa, Figure 3b). The storage modulus of these blends at 25 °C was low for all samples (<200 MPa, Figure S6). However, when the molecular weight of P4VP is significantly higher than its M_e, the blend with the highest H-bonding fraction (**MAA5-P4VP5 (60K)**) became much more rigid. It has an impressive 17 MPa of tensile strength. This value is substantial, given the simplicity of processing and easy availability of materials. Additionally, this blend sample also exhibited the highest storage modulus of 390 MPa at 25 °C. Under low fraction of H-bonding components (4 wt %), this blend system with **P4VP-60** did not show much difference with those using low molecular weight P4VP (**MAA2-P4VP2 (8K)** vs **MAA2-P4VP2 (60K)**). In both cases, only soft and partially elastic bioplastics were obtained. Additionally, DMA tests indicated that all samples underwent complete slippage at high temperature and never reached a rubbery plateau (Figure S6). The determination of T_g by DMA turned out to be difficult. Though H-bonding significantly increased the tensile strength and modulus of blends at room temperature, it weakened appreciably at higher temperature (over 50–60 °C). Most blends started to melt and became viscoelastic.

DOI: 10.1021/acs.macromol.9b01828
Macromolecules 2019, 52, 8967–8975

Table 3. Mechanical Properties of H-Bonded Polymer Blends with Varied Acid Monomers[a]

sample code (wt %)	M_n (Da) (P4VP)	T_g[b] (°C)	stress at break (MPa)	strain at break (%)	toughness (MJ/m^3)	storage modulus at 25 °C (MPa)
AA2-P4VP2 (60K)	60000	−2	1.1 ± 0.01	433 ± 5	4.6 ± 0.4	35
AA2-P4VP5 (60K)	60000	1	3.2 ± 0.1	315 ± 11	8.5 ± 0.2	
AA5-P4VP2 (60K)	60000	3	8.2 ± 0.2	208 ± 2	14.4 ± 0.2	
AA5-P4VP5 (60K)	60000	8	11.9 ± 0.5	143 ± 4	15.5 ± 0.1	280
CEA2-P4VP2 (60K)	60000	−4	3.5 ± 0.05	328 ± 13	8.9 ± 0.2	95
CEA2-P4VP5 (60K)	60000	−1	7.7 ± 0.5	272 ± 9	9.6 ± 0.0	
CEA5-P4VP2 (60K)	60000	1	10.8 ± 0.3	238 ± 7	14.9 ± 0.0	
CEA5-P4VP5 (60K)	60000	5	15.0 ± 0.2	112 ± 3	12.7 ± 0.1	140

[a]All blends use the following naming system: the copolymer name indicating the acid monomer and its weight fraction in number (**AA2**, **AA5**, **CEA2**, or **CEA5**) and P4VP following by a number indicating its weight fraction. The number in parentheses refers to as the molecular weight P4VP. [b]T_g values were obtained via DSC (second heating cycle).

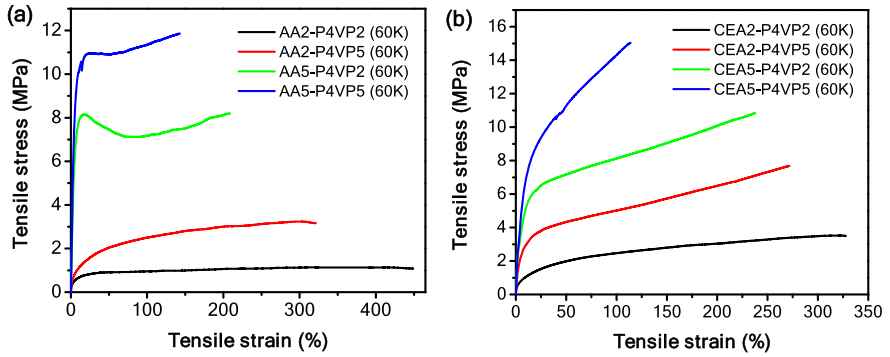

Figure 4. Stress−strain curves of polymer blends with variation in acid monomers used as H-bonding donors: (a) AA copolymers; (b) CEA copolymers.

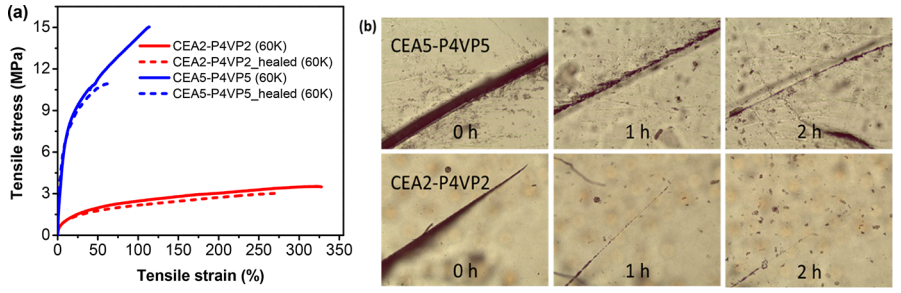

Figure 5. Self-healing of polymer blends: (a) stress−strain curves of polymer blends, **CEA2-P4VP2 (60K)** and **CEA5-P4VP5 (60K)**, before and after healing; (b) optical microscopy images of polymer blends heated at 50 °C over 2 h.

Given the initial investigation, we concluded that the presence of highly entangled P4VP (high M_n) could serve as efficient chain entanglement. We then focused on the use of P4VP with M_n = 60000 Da for further studies. In next steps, we considered to tune the compositions of H-bonding donors: the structures of acids. PAA is much more elastic than PMAA. The blends with MAA as H-bonding donors are rigid but very brittle. This is not surprising as these polymers are all glassy at room temperature (25 °C) with their T_gs in the range 30−40 °C. We hypothesized that with the introduction of acrylic acid-type donors it is possible to prepare rigid and tough bioplastics. Table 3 lists mechanical properties of another set of blend systems with AA as comonomer unit with soybean monomer.

According to differential scanning calorimetry (DSC), the T_gs (−2 to 4 °C) in new copolymers P(SBMA-*co*-AA) are much lower than those (19−35 °C) in P(SBMA-*co*-MAA) with acid donors in the range 2−5 wt %. Once blended with P4VP, the T_gs of these AA blends remained low (<10 °C), indicating they would be significantly more rubbery and elastic at room temperature than their brittle, higher T_g MAA counterparts. In the blend with P4VP (60K), a low fraction of H-bonding components (i.e., 4 wt % in **AA2-P4VP2**), only a soft and elastic polymer was obtained (Figure 4a). When the fraction increases to 10 wt %, the blend has tensile strength and strain-at-break respectively at ∼12 MPa and ∼140%. In addition, it was observed with almost 20 times increase in toughness compared with an equivalent blend using MAA (15.5 vs 0.8 MJ/m^3).

Given the long pendant fatty chains on SBMA units, there was a concern whether the small AA units could be deeply surrounded by SBMA, leading to insufficient H-bonding interactions between the acid and pyridine groups.[47] To overcome such steric hindrance, a longer acid monomer, CEA, was used. These P(SBMA-*co*-CEA) copolymers are the softest among the three acid systems due to their ductile backbone and longer, flexible side chain with low T_g ($T_g \leq 5$ °C, Table 3). It turned out that this set of blend systems showed enhanced toughness (Figure 4b), especially when the fractions

DOI: 10.1021/acs.macromol.9b01828
Macromolecules 2019, 52, 8967−8975

of H-bonding components are low. A blend with only 4 wt % of CEA and 4VP possesses tensile strength as high as 3.5 MPa, about 3 times of the AA-based blend system. A similar increase in mechanical properties of this sample was observed by DMA (Table 3 and Figure S6), which has storage modulus of ∼100 MPa, the highest among all blends with 4 wt % H-bonding components. For the blend with 10 wt % H-bonding components (**CEA5-P4VP5 (60K)**), it displayed as a tough and elastic bioplastic, with tensile strength and strain-at-break respectively at ∼15 MPa and ∼112%.

Self-Healing Properties. Reversible bonds, including H-bonding, have been utilized extensively in self-healing polymeric systems.[34,51−53] Because of the presence of supramolecular polymer networks in the blends, self-healing properties were expected. To test the self-healing of these blends, films were placed into an oven at 50 °C, above the T_g of these materials and at which the H-bonding is in the process of weakening (from SAXS data). Optical microscopy was used to monitor the self-healing. Images were taken directly every hour until full healing was observed (Figure 5). Both CEA-containing copolymers, **CEA2-P4VP2 (60K)** and **CEA5-P4VP5 (60K)**, appeared visually mended almost completely after 2 h, though the former self-healed faster due to the low level of H-bonding. Additionally, tensile testing was used to evaluate the recovery of mechanical properties. Overall, both films exhibited a decrease in elasticity and toughness, observed by a decrease in tensile stress and strain at break. When tested, other films from MAA- and AA-containing copolymers could not mend even under higher temperature (80 °C) and longer time (>48 h), indicating the critical role of structures of H-bonding donors.

DISCUSSION

Among various strategies we have developed to improve mechanical properties of biobased polymers, the "supramolecular chain entanglement" strategy is aimed to combine simplicity and robustness. It must consider both economics and sustainability. By varying a few simple structural components in the polymer blends, including carboxylic acids, molecular weight of entangling polymers, and the level of H-bonding, the physically cross-linked supramolecular microstructures can be well controlled, leading to highly tailorable thermomechanical properties. We believe there are three major compositions that could be tuned toward manipulation of mechanical properties of the polymeric systems in this work, as illustrated in Figure 6.

Level of Physical Cross-Linking via H-Bonding (Figure 6a). The goal in designing simple supramolecular H-bonding is to achieve physical cross-linking, which could overcome the poor entanglement of matrix polymers. One could utilize other H-bonding systems with much stronger association such as quadrupole H-bonding. However, the economics must be considered in the design. Additionally, the H-bonding fractions of carboxylic acids and pyridine need to be balanced. The lower fraction leads to soft blends, while the higher composition results in brittle bioplastics. In addition, the biomass component should be maximally used. In the current blend systems, a range of fractions from 4 to 10 wt % seem to be sufficient to induce various levels of physical cross-links that significantly enhance chain entanglements compared with simple soybean oil-derived homopolymers.

Molecular Weight of Chain-Entangling Polymers (Figure 6b). The chain-entangling polymer essentially serves as a type of entanglement to wrap around biobased polymers, in addition to physical cross-linking via H-bonding. It is highly preferred that both physical phenomena corroborate with each other. It is believed that P4VP could achieve both roles in this system, providing its inherent entangling ability and "chain entanglement" via its pyridine as a H-bonding acceptor. Therefore, the entanglement present inherently in the P4VP portion of this system is important to the mechanical properties of polymer blends. When low molecular weight P4VP (8 kDa) is used, well below its M_e (∼30 kDa), the effect of chain entanglement would be minimal. Under this scenario, the possible entanglement of PSMBA polymers could be only assisted by the presence of H-bonding. As a result, mechanical properties are mostly inferior (Figure 3b). When the M_n of P4VP is increased to 30 kDa and then to 60 kDa, the increasing entanglement of P4VP and therefore chain entanglement enables the ability to dissipate stress in the blends, resulting in mechanical enhancement.

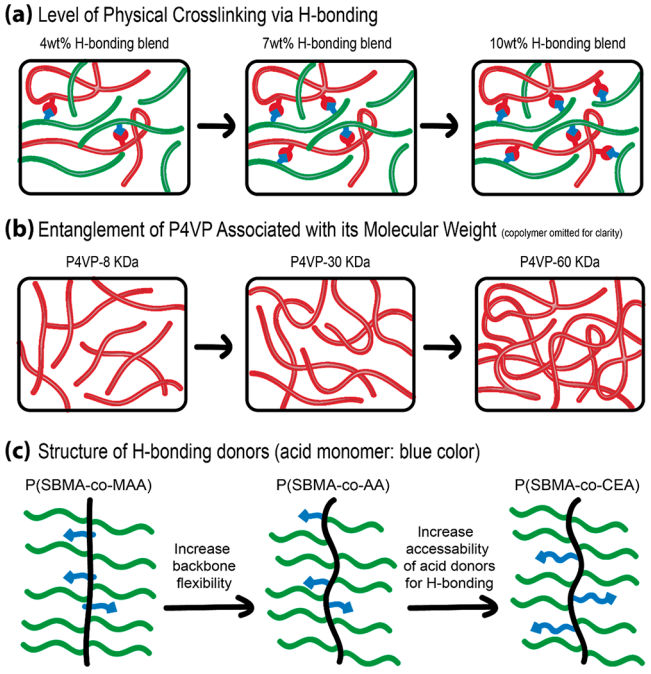

Figure 6. Illustration of varying chemical compositions on the molecular interactions of polymer blends: (a) level of physical cross-linking via H-bonding; (b) entanglement by P4VP by changing its molecular weight; (c) structures of H-bonding honors (acid monomers).

Chemical Structures of H-Bonding Donors (Figure 6c). The structures for H-bonding donors not only control the physical cross-linking but also dictate the chain rigidity. With the use of carboxylic acids, methacrylic comonomer (MAA) significantly increases the rigidity of copolymer, P(SBMA-*co*-MAA), resulting in fragility of polymer blends. These blends behave like glassy thermoplastics with low strain-at-break. When the copolymer backbone is softened by using acrylic comonomer (AA), blends have more flexibility for chain movement and are observed with more rubbery properties (much higher strain at break and thus increased toughness). Lastly, the softest and most ductile copolymer, P(SBMA-*co*-CEA), contains a soft backbone and a flexible side chain. In addition to having benefits similar to AA copolymer, the flexible side chain would facilitate more efficient H-bonding. Combining all together, CEA-containing blends exhibit higher

DOI: 10.1021/acs.macromol.9b01828
Macromolecules 2019, 52, 8967−8975

strength, strain, and toughness under all fractions of H-bonding compared with those of MAA and AA counterparts.

CONCLUSIONS

In summary, this work demonstrated a new concept of "supramolecular chain entanglement" that exploits H-bonding and physical entangling to improve thermomechanical properties of biobased polymers. Simple radical copolymerization was employed for soybean oil-derived fatty monomer and (meth)-acylic acid, the latter of which serves as H-bonding donor to interact with a pyridine-based polymer that additionally provides chain entanglement around unentangled fatty polymers. Despite poor chain entanglement of plant oil-based homopolymers, control of macromolecular compositions in these polymer blends was achieved through tuning acid donor structures, molecular weight of chain entangling polymers, and the level of H-bonding. The dual effects of H-bonding and chain entanglement enable a substantial enhancement in mechanical properties of biobased polymers. Given the availability of versatile supramolecular interactions together with the ease of synthesis and atom economics, this strategy could pave a new path to accessing high performance sustainable polymers and materials from renewable resources.

EXPERIMENTAL SECTION

Materials. Plenish high oleic soybean oil (HOSO) was provided by Pioneer. Azobis(isobutyronitrile) (AIBN, 98%, Aldrich) was recrystallized from methanol. 4-Vinylpyridine (Sigma, 96%) was vacuum-distilled. Other monomers were run through basic alumina to remove inhibitors. All other reagents were from commercial resources and used as received unless otherwise mentioned. SBMA and PSBMA were synthesized following previously published procedures.[54]

Synthesis of Copolymers (P(SBMA-co-MAA), P(SBMA-co-AA), and P(SBMA-co-CEA)). The following procedure was used for **MAA5**; similar procedures were followed for all other copolymers. SBMA (7 g, 0.017 mol), MAA (0.33 g, 0.0035 mol), and AIBN (35 mg, 0.21 mmol) were placed in a 50 mL round-bottom flask and dissolved in toluene (14 mL). The flask was sealed, purged with nitrogen for 15 min, and placed in an 80 °C oil bath. After 16 h, the polymer was poured into cold methanol. The resulting polymer was precipitated twice into methanol and dried for 24 h in a 50 °C vacuum oven.

Synthesis of Poly(4-vinylpyridine). The following procedure was used to synthesize **P4VP-30**. A similar procedure was followed for other molecular weights. 4-Vinylpyridine (5.97 g, 56.9 mmol) and 4-cyano-4-(thiobenzoylthio)pentanoic acid (42 mg, 0.15 mmol) were placed in a 25 mL Schlenk flask. AIBN (1.23 mg, 0.0075 mmol) was dissolved in THF (0.1 mL) and added to the flask. The flask was sealed and purged of oxygen using three cycles of freeze–pump–thaw. The flask was placed in a 60 °C oil bath. The polymer was dissolved into hexane and precipitated in diethyl ether three times. The polymer was dried in a 60 °C oven for 24 h.

Characterization. ^{1}H NMR spectra were recorded on a Varian Mercury 300 spectrometer in deuterated chloroform ($CDCl_3$) with tetramethylsilane (TMS) as an internal reference. Solid state ^{13}C CP-MAS spectra were collected on a Bruker Avance III-HD 500 MHz (^{13}C frequency of 129.79 MHz) spectrometer fitted with a 1.9 mm MAS probe. The spectra were collected at ambient temperature with sample rotation rate of 20 kHz. A 2 ms contact time with linear ramping on the ^{1}H channel and a 62.5 kHz field on the ^{13}C channel were used for cross-polarization. ^{1}H dipolar decoupling was performed with SPINAL64 modulation and 145 kHz field strength. Free induction decays were collected with a 20 ms acquisition time over a 350 ppm spectra width with a relaxation delay of 2 s. The molecular weight and molecular weight distribution of polymers were determined by gel permeation chromatography (GPC) equipped with a 2414 RI detector, a 1525 binary pump and three Styragel columns. The columns consisted of HR 1, HR 3, and HR 5E with effective molecular weight ranges of 100–5K, 500–30K, and 2K–4M, respectively. THF was used as eluent at 35 °C with a flow rate of 1.0 mL/min. The system was calibrated with polystyrene standards obtained from Polymer Laboratories. GPC samples were prepared by dissolving the sample in THF with a concentration of 3.0 mg/mL and passing through microfilters with a pore size of 0.2 μm. The glass transition temperature (T_g) of polymers was determined by using differential scanning calorimetry (DSC) conducted on a DSC 2000 instrument (TA Instruments). Samples were first heated from −70 to +200 °C at a rate of 10 °C/min. After cooling to −70 °C at the same rate, the data were collected from the second heating and cooling scan. About 10 mg of each sample was used for the DSC test with nitrogen gas at a flow rate of 50 mL/min. Thermogravimetric analysis (TGA) was conducted on a Q5000 TGA system (TA Instruments), ramping from 25 to 600 °C with a rate of 10 °C/min. About 10 mg of sample is used per test. Tensile stress–strain testing was performed with an Instron 5543A testing instrument with a cross-head speed of 20 mm/min. Five replicate samples from different films were used to obtain an average value for each. The error was calculated from standard deviation by using data collected from all five replicate samples. Fourier transform infrared spectrometry (FTIR) spectra were taken on a PerkinElmer spectrum 100 FTIR spectrometer. Variable temperature FT-IR (VT-FTIR) experiments were performed on a Bruker Tensor 27 FT-IR spectrophotometer with a Eurotherm 2404 temperature controller. Dried polymer films were used for measurement. Dynamic thermomechanical analysis (DMA) was performed by using a Q800 DMA (TA Instruments). The DMA spectra were scanned with a frequency of 1 Hz and a heating rate of 3 °C/min. Small-angle X-ray scattering (SAXS) experiments were conducted by using SAXSLab Ganesha at the South Carolina SAXS Collaborative at the University of South Carolina. A Xenocs GeniX3D microfocus source was used with a copper target to generate a monochromic beam with a 0.154 nm wavelength. The instrument was calibrated by using a silver behenate reference with the first-order scattering vector $q^* = 1.076$ nm^{-1}, with $q = 4\pi\lambda^{-1} \sin\theta$, where λ is the X-ray wavelength and 2θ is the total scattering angle. A 300 K Pilatus detector (Dectris) was used to collect the two-dimensional (2D) SAXS patterns. Radial integration of 2D patterns reduced the data to 1D profiles. Polymer films were fixed to a mount such that only the sample was measured at the exclusion of any mounting tape. All data were acquired for about 0.5 h at room temperature with an incident X-ray flux of ∼1.5M photons per second. Temperature-dependent SAXS measurements were taken using a Linkam Scientific Instrument HFS350X-GI hot stage in a SAXSLab Ganesha. The sample was heated at a rate of 10 °C/min and left to equilibrate for 10 min. Cooling of the sample to room temperature was performed at a rate of 5 °C/min.

Mechanical Properties. Films for tensile testing were prepared by dissolving 0.75 g of a copolymer and various amounts of P4VP in 10 mL of chloroform. The solution was sonicated for 5 min and poured in a PTFE mold. After the evaporation of solvent over 48 h, the film was put under vacuum for 12 h at room temperature and then 12 h at 60 °C. Dog-bone-shaped specimens were cut from the cast film with a length of 20 mm and a width of 5.0 mm. The thickness was measured prior to each measurement. Testing occurred at room temperature with a crosshead speed of 20 mm/min.

ASSOCIATED CONTENT

Supporting Information

The Supporting Information is available free of charge on the ACS Publications website at DOI: 10.1021/acs.macromol.9b01828.

^{1}H NMR spectra of PSBMA and copolymers (Figure S1), GPC traces of P4VP homopolymers (Figure S2), FTIR spectra of copolymers and blends (Figure S3), ^{13}C solid-state CP-MAS NMR spectra (Figure S4), SAXS profiles of copolymer and blends (Figure S5), DMA

DOI: 10.1021/acs.macromol.9b01828
Macromolecules 2019, 52, 8967–8975

curves of polymer blends (Figure S6), complete weight and molar fractions of all components in each polymer blend (Table S1), TGA curves of copolymers and blends (Figure S7), and stress−strain curves of blends (Figure S8) (PDF)

AUTHOR INFORMATION

Corresponding Author

*E-mail tang4@mailbox.sc.edu.

ORCID

Meghan E. Lamm: 0000-0003-3485-4322
Zhongkai Wang: 0000-0003-1842-1260
Md Anisur Rahman: 0000-0002-7190-9751
Benjamin Lamm: 0000-0003-4041-7786
Chuanbing Tang: 0000-0002-0242-8241

Notes

The authors declare no competing financial interest.

ACKNOWLEDGMENTS

This work was supported by the National Science Foundation (DMR-1806792).

REFERENCES

(1) Biermann, U.; Bornscheuer, U.; Meier, M. A.; Metzger, J. O.; Schafer, H. J. Oils and Fats as Renewable Raw Materials in Chemistry. *Angew. Chem., Int. Ed.* **2011**, *50*, 3854−3871.

(2) Raquez, J. M.; Deléglise, M.; Lacrampe, M. F.; Krawczak, P. Thermosetting (Bio)Materials Derived from Renewable Resources: A Critical Review. *Prog. Polym. Sci.* **2010**, *35*, 487−509.

(3) Schneiderman, D. K.; Hillmyer, M. A. 50th Anniversary Perspective: There Is a Great Future in Sustainable Polymers. *Macromolecules* **2017**, *50*, 3733−3750.

(4) Wang, Z.; Yuan, L.; Tang, C. Sustainable Elastomers from Renewable Biomass. *Acc. Chem. Res.* **2017**, *50*, 1762−1773.

(5) Zhu, Y.; Romain, C.; Williams, C. K. Sustainable Polymers from Renewable Resources. *Nature* **2016**, *540*, 354−362.

(6) Lambert, S.; Wagner, M. Environmental Performance of Bio-Based and Biodegradable Plastics: The Road Ahead. *Chem. Soc. Rev.* **2017**, *46*, 6855−6871.

(7) Yao, K.; Tang, C. Controlled Polymerization of Next-Generation Renewable Monomers and Beyond. *Macromolecules* **2013**, *46*, 1689−1712.

(8) Hong, M.; Chen, E. Y. X. Chemically Recyclable Polymers: A Circular Economy Approach to Sustainability. *Green Chem.* **2017**, *19*, 3692−3706.

(9) Yu, J.; Wang, J.; Wang, C.; Liu, Y.; Xu, Y.; Tang, C.; Chu, F. Uv-Absorbent Lignin-Based Multi-Arm Star Thermoplastic Elastomers. *Macromol. Rapid Commun.* **2015**, *36*, 398−404.

(10) Gandini, A.; Lacerda, T. M.; Carvalho, A. J.; Trovatti, E. Progress of Polymers from Renewable Resources: Furans, Vegetable Oils, and Polysaccharides. *Chem. Rev.* **2016**, *116*, 1637−1669.

(11) Isikgor, F. H.; Becer, C. R. Lignocellulosic Biomass: A Sustainable Platform for the Production of Bio-Based Chemicals and Polymers. *Polym. Chem.* **2015**, *6*, 4497−4559.

(12) Cornille, A.; Auvergne, R.; Figovsky, O.; Boutevin, B.; Caillol, S. A Perspective Approach to Sustainable Routes for Non-Isocyanate Polyurethanes. *Eur. Polym. J.* **2017**, *87*, 535−552.

(13) Lligadas, G.; Ronda, J. C.; Galià, M.; Cádiz, V. Renewable Polymeric Materials from Vegetable Oils: A Perspective. *Mater. Today* **2013**, *16*, 337−343.

(14) Miao, S.; Wang, P.; Su, Z.; Zhang, S. Vegetable-Oil-Based Polymers as Future Polymeric Biomaterials. *Acta Biomater.* **2014**, *10*, 1692−1704.

(15) Montero de Espinosa, L.; Meier, M. A. R. Plant Oils: The Perfect Renewable Resource for Polymer Science?! *Eur. Polym. J.* **2011**, *47*, 837−852.

(16) Ronda, J. C.; Lligadas, G.; Galià, M.; Cádiz, V. Vegetable Oils as Platform Chemicals for Polymer Synthesis. *Eur. J. Lipid Sci. Technol.* **2011**, *113*, 46−58.

(17) Desroches, M.; Escouvois, M.; Auvergne, R.; Caillol, S.; Boutevin, B. From Vegetable Oils to Polyurethanes: Synthetic Routes to Polyols and Main Industrial Products. *Polym. Rev.* **2012**, *52*, 38−79.

(18) Wool, R. P. Polymer Entanglements. *Macromolecules* **1993**, *26*, 1564−1569.

(19) Ding, W.; Wang, S.; Yao, K.; Ganewatta, M. S.; Tang, C.; Robertson, M. L. Physical Behavior of Triblock Copolymer Thermoplastic Elastomers Containing Sustainable Rosin-Derived Polymethacrylate End Blocks. *ACS Sustainable Chem. Eng.* **2017**, *5*, 11470−11480.

(20) Ganewatta, M. S.; Ding, W.; Rahman, M. A.; Yuan, L.; Wang, Z.; Hamidi, N.; Robertson, M. L.; Tang, C. Biobased Plastics and Elastomers from Renewable Rosin Via "Living" Ring-Opening Metathesis Polymerization. *Macromolecules* **2016**, *49*, 7155−7164.

(21) Wang, S.; Kesava, S. V.; Gomez, E. D.; Robertson, M. L. Sustainable Thermoplastic Elastomers Derived from Fatty Acids. *Macromolecules* **2013**, *46*, 7202−7212.

(22) Rahman, M. A.; Lokupitiya, H. N.; Ganewatta, M. S.; Yuan, L.; Stefik, M.; Tang, C. Designing Block Copolymer Architectures toward Tough Bioplastics from Natural Rosin. *Macromolecules* **2017**, *50*, 2069−2077.

(23) Wang, Z.; Yuan, L.; Trenor, N. M.; Vlaminck, L.; Billiet, S.; Sarkar, A.; Du Prez, F. E.; Stefik, M.; Tang, C. Sustainable Thermoplastic Elastomers Derived from Plant Oil and Their "Click-Coupling" Via Tad Chemistry. *Green Chem.* **2015**, *17*, 3806−3818.

(24) Nasiri, M.; Reineke, T. M. Sustainable Glucose-Based Block Copolymers Exhibit Elastomeric and Adhesive Behavior. *Polym. Chem.* **2016**, *7*, 5233−5240.

(25) Shin, J.; Lee, Y.; Tolman, W. B.; Hillmyer, M. A. Thermoplastic Elastomers Derived from Menthide and Tulipalin A. *Biomacromolecules* **2012**, *13*, 3833−3840.

(26) Gallagher, J. J.; Hillmyer, M. A.; Reineke, T. M. Acrylic Triblock Copolymers Incorporating Isosorbide for Pressure Sensitive Adhesives. *ACS Sustainable Chem. Eng.* **2016**, *4*, 3379−3387.

(27) Nasiri, M.; Saxon, D. J.; Reineke, T. M. Enhanced Mechanical and Adhesion Properties in Sustainable Triblock Copolymers Via Non-Covalent Interactions. *Macromolecules* **2018**, *51*, 2456−2465.

(28) Yuan, L.; Wang, Z.; Ganewatta, M. S.; Rahman, M. A.; Lamm, M. E.; Tang, C. A Biomass Approach to Mendable Bio-Elastomers. *Soft Matter* **2017**, *13*, 1306−1313.

(29) Song, L.; Wang, Z.; Lamm, M. E.; Yuan, L.; Tang, C. Supramolecular Polymer Nanocomposites Derived from Plant Oils and Cellulose Nanocrystals. *Macromolecules* **2017**, *50*, 7475−7483.

(30) Brunsveld, L.; Folmer, B. J. B.; Meijer, E. W.; Sijbesma, R. P. Supramolecular Polymers. *Chem. Rev.* **2001**, *101*, 4071−4097.

(31) Yang, L.; Tan, X.; Wang, Z.; Zhang, X. Supramolecular Polymers: Historical Development, Preparation, Characterization, and Functions. *Chem. Rev.* **2015**, *115*, 7196−7239.

(32) Pollino, J. M.; Weck, M. Non-Covalent Side-Chain Polymers: Design Principles, Functionalization Strategies, and Perspectives. *Chem. Soc. Rev.* **2005**, *34*, 193−207.

(33) Zhang, Z. P.; Rong, M. Z.; Zhang, M. Q. Polymer Engineering Based on Reversible Covalent Chemistry: A Promising Innovative Pathway Towards New Materials and New Functionalities. *Prog. Polym. Sci.* **2018**, *80*, 39−93.

(34) Yang, Y.; Urban, M. W. Self-Healing Polymeric Materials. *Chem. Soc. Rev.* **2013**, *42*, 7446−7467.

(35) Chen, L. J.; Yang, H. B. Construction of Stimuli-Responsive Functional Materials Via Hierarchical Self-Assembly Involving Coordination Interactions. *Acc. Chem. Res.* **2018**, *51*, 2699−2710.

(36) Heinzmann, C.; Weder, C.; de Espinosa, L. M. Supramolecular Polymer Adhesives: Advanced Materials Inspired by Nature. *Chem. Soc. Rev.* **2016**, *45*, 342−358.

DOI: 10.1021/acs.macromol.9b01828
Macromolecules 2019, 52, 8967−8975

(37) Liu, J.; Tan, C. S.; Yu, Z.; Lan, Y.; Abell, C.; Scherman, O. A. Biomimetic Supramolecular Polymer Networks Exhibiting Both Toughness and Self-Recovery. *Adv. Mater.* **2017**, *29*, 1604951.
(38) Razgoniaev, A. O.; Mikhailov, K. I.; Obrezkov, F. A.; Butaeva, E. V.; Ostrowski, A. D. Supramolecular Elastomers: Switchable Mechanical Properties and Tuning Photohealing with Changes in Supramolecular Interactions. *J. Polym. Sci., Part A: Polym. Chem.* **2018**, *56*, 1003−1011.
(39) Deng, Y.; Wang, T.; Guo, Y.; Qiu, X.; Qian, Y. Layer-by-Layer Self-Assembled Films of a Lignin-Based Polymer through Hydrogen Bonding. *ACS Sustainable Chem. Eng.* **2015**, *3*, 1215−1220.
(40) Shimizu, L. S. Perspectives on Main-Chain Hydrogen Bonded Supramolecular Polymers. *Polym. Int.* **2007**, *56*, 444−452.
(41) Sontjens, S. H. M.; Renken, R. A. E.; van Gemert, G. M. L.; Engels, T. A. P.; Bosman, A. W.; Janssen, H. M.; Govaert, L. E.; Baaijens, F. P. T. Thermoplastic Elastomers Based on Strong and Well-Defined Hydrogen-Bonding Interactions. *Macromolecules* **2008**, *41*, 5703−5708.
(42) He, Y.; Zhu, B.; Inoue, Y. Hydrogen Bonds in Polymer Blends. *Prog. Polym. Sci.* **2004**, *29*, 1021−1051.
(43) Lee, J. Y.; Painter, P. C.; Coleman, M. M. Hydrogen Bonding in Polymer Blends. 4. Blends Involving Polymers Containing Methacrylic Acid and Vinylpyridine Groups. *Macromolecules* **1988**, *21*, 954−960.
(44) Lamm, M. E.; Li, P.; Hankinson, S.; Zhu, T.; Tang, C. Plant Oil-Derived Copolymers with Remarkable Post-Polymerization Induced Mechanical Enhancement for High Performance Coating Applications. *Polymer* **2019**, *174*, 170−177.
(45) Yuan, L.; Wang, Z.; Trenor, N. M.; Tang, C. Amidation of Triglycerides by Amino Alcohols and Their Impact on Plant Oil-Derived Polymers. *Polym. Chem.* **2016**, *7*, 2790−2798.
(46) Yuan, L.; Wang, Z.; Trenor, N. M.; Tang, C. Robust Amidation Transformation of Plant Oils into Fatty Derivatives for Sustainable Monomers and Polymers. *Macromolecules* **2015**, *48*, 1320−1328.
(47) Coleman, M. M.; Pehlert, G. J.; Painter, P. C. Functional Group Accessibility in Hydrogen Bonded Polymer Blends. *Macromolecules* **1996**, *29*, 6820−6831.
(48) Convertine, A. J.; Sumerlin, B. S.; Thomas, D. B.; Lowe, A. B.; McCormick, C. L. Synthesis of Block Copolymers of 2- and 4-Vinylpyridine by Raft Polymerization. *Macromolecules* **2003**, *36*, 4679−4681.
(49) Coleman, M. M.; Painter, P. C. Hydrogen Bonded Polymer Blends. *Prog. Polym. Sci.* **1995**, *20*, 1−59.
(50) Akbey, Ü.; Graf, R.; Peng, Y. G.; Chu, P. P.; Spiess, H. W. Solid-State Nmr Investigations of Anhydrous Proton-Conducting Acid−Base Poly(Acrylic Acid)− Poly(4-Vinyl Pyridine) Polymer Blend System: A Study of Hydrogen Bonding and Proton Conduction. *J. Polym. Sci., Part B: Polym. Phys.* **2009**, *47*, 138−155.
(51) Sahu, P.; Bhowmick, A. K. Sustainable Self-Healing Elastomers with Thermoreversible Network Derived from Biomass Via Emulsion Polymerization. *J. Polym. Sci., Part A: Polym. Chem.* **2019**, *57*, 738−751.
(52) Bossion, A.; Olazabal, I.; Aguirresarobe, R. H.; Marina, S.; Martín, J.; Irusta, L.; Taton, D.; Sardon, H. Synthesis of Self-Healable Waterborne Isocyanate-Free Poly(Hydroxyurethane)-Based Supramolecular Networks by Ionic Interactions. *Polym. Chem.* **2019**, *10*, 2723−2733.
(53) Comí, M.; Lligadas, G.; Ronda, J. C.; Galià, M.; Cádiz, V. Adaptive Bio-Based Polyurethane Elastomers Engineered by Ionic Hydrogen Bonding Interactions. *Eur. Polym. J.* **2017**, *91*, 408−419.
(54) Yuan, L.; Wang, Z. K.; Trenor, N. M.; Tang, C. B. Robust Amidation Transformation of Plant Oils into Fatty Derivatives for Sustainable Monomers and Polymers. *Macromolecules* **2015**, *48*, 1320−1328.

DOI: 10.1021/acs.macromol.9b01828
Macromolecules 2019, 52, 8967−8975